1-1-2009

Late Neoproterozoic passive margin of East Gondwana: geochemical constraints from the Anakie Inlier, central Queensland, Australia

Christopher L. Fergusson
University of Wollongong, cferguss@uow.edu.au

R Offler
University of Newcastle

T Green
University of Wollongong

Recommended Citation
Fergusson, Christopher L.; Offler, R; and Green, T: Late Neoproterozoic passive margin of East Gondwana: geochemical constraints from the Anakie Inlier, central Queensland, Australia 2009, 301-312.
https://ro.uow.edu.au/scipapers/3022

Late Neoproterozoic passive margin of East Gondwana: geochemical constraints from the Anakie Inlier, central Queensland, Australia

Abstract

Development of the East Gondwana passive margin and when it occurred are constrained by the composition of low grade mafic schists and U-Pb ages of detrital zircons in psammitic schists from the Bathampton Metamorphics in the Anakie Inlier of central Queensland. These rocks show considerable variation in light lithophile elements due to post-magmatic processes. They have flat heavy rare earth element patterns, low-TiO_2 (<2 >wt%) contents and their immobile element Ti, V, Y, La, Nb, Th and Zr values, indicate that they have an NMORB- like magmatic affinity. However, they differ from N-MORB in that they show light rare earth depleted patterns and lower incompatible trace element contents. Their relative low abundance and association with metasediments suggest they formed in a magma-poor rifted margin setting. They are associated with psammitic rocks with detrital zircon ages indicating probable deposition in the late Neoproterozoic at ca 600 Ma. A magma-poor rifted margin in northeastern Australia differs from the volcanic passive setting that occurred in southeastern Australia at this time. These findings support development of the East Gondwana margin at 600 Ma that may have been related to rifting of a microcontinent off East Gondwana well after the breakup of Rodinia at ca 750 Ma.

Keywords

Late, Neoproterozoic, passive, margin, East, Gondwana, geochemical, constraints, from, Anakie, Inlier, central, Queensland, Australia, GeoQUEST

Disciplines

Life Sciences | Physical Sciences and Mathematics | Social and Behavioral Sciences

Publication Details

Fergusson, C. L., Offler, R. and Green, T. J. (2009). Late Neoproterozoic passive margin of East Gondwana: geochemical constraints from the Anakie Inlier, central Queensland, Australia. Precambrian Research, 168 (3-4), 301-312.

Late Neoproterozoic passive margin of East Gondwana: geochemical constraints from the Anakie Inlier, central Queensland, Australia

C. L. Fergusson[a,*], R. Offler[b], T.J. Green[a,c]

[a]*School of Earth and Environmental Sciences, University of Wollongong NSW 2522, Australia*
[b]*Discipline of Earth Sciences, School of Environmental & Life Sciences, University of Newcastle, Callaghan, NSW 2308, Australia*
[c]*Present address: 8 Hare Street, Lamington, WA 6450, Australia*

Received , received in revised form , accepted

Abstract

Development of the East Gondwana passive margin and when it occurred are constrained by the composition of low grade mafic schists and U-Pb ages of detrital zircons in psammitic schists from the Bathampton Metamorphics in the Anakie Inlier of central Queensland. These rocks show considerable variation in light lithophile elements due to post-magmatic processes. They have flat heavy rare earth element patterns, low-TiO_2 (<2 wt%) contents and their immobile element Ti, V, Y, La, Nb, Th and Zr values, indicate that they have an N-MORB-like magmatic affinity. However, they differ from N-MORB in that they show light rare earth depleted patterns and lower incompatible trace element contents. Their relative low abundance and association with metasediments suggest they formed in a magma-poor rifted margin setting. They are associated with psammitic rocks with detrital zircon ages indicating probable deposition in the late Neoproterozoic at ca 600 Ma. A magma-poor rifted margin in northeastern Australia differs from the volcanic passive setting that occurred in southeastern Australia at this time. These findings support development of the East Gondwana margin at 600 Ma that may have been related to rifting of a microcontinent off East Gondwana well after the breakup of Rodinia at ca 750 Ma.

Key words: Anakie Inlier; East Gondwana; N-MORB; Australia; passive margin

1. Introduction

The development of the East Gondwana passive margin is unclear as to timing of rifting, fragmentation and the number and identity of continents that formed the conjugate margin. Some authors favour breakup at around 800 Ma on the basis of palaeomagnetic constraints, the development of the 827 Ma Gairdner dyke swarm in the northeastern Gawler craton and rifting in the Delamerian Orogen, which includes the Adelaide Rift Complex, of South Australia (Fig. 1; Wingate *et al*. 1998; Pisarevsky *et al*. 2003). Other authors argue that continental fragmentation and passive margin development for East Gondwana was around

[*]Corresponding author
E-mail address: cferguss@uow.edu.au
Telephone: 61242213860
Fax: 61242214250

560 Ma consistent with a 400 m.y. cycle of supercontinent agglomeration and fragmentation (Veevers *et al*. 1997; Veevers 2000). A volcanic passive margin is now recognised in southeastern Australia after continental fragmentation at around 600 Ma (Direen & Crawford 2003a, b). Igneous activity included a mildly alkaline volcanic succession in the Wonominta Block of western New South Wales, and eruption of tholeiitic rocks in western Victoria and western Tasmania (Crawford *et al*. 2003; Direen & Crawford 2003a, b; Meffre *et al*. 2004).

Evidence for passive margin development should be elsewhere in East Gondwana such as in the Thomson Fold Belt of Queensland and in the Transantarctic Mountains of East Antarctica (Fig. 2). In the central Transantarctic Mountains, the Beardmore Group represents extension, magmatism and sedimentation at ca 670 Ma based on a zircon U-Pb age on the Cotton Plateau Gabbro (Fig. 2; Goodge *et al*. 2002, 2004a). In the Ross Orogen siliciclastic deposits dominated during the Cambrian and were sourced from an active convergent margin that developed over the older rifted and passive margin at ca 580 Ma (Goodge *et al*. 2002, 2004a, b). Thus the passive margin and associated minor mafic igneous rocks formed at least ca 70 m.y. earlier than in southeastern Australia.

In central Queensland, the Anakie Inlier includes an older succession (ca 600 Ma) containing mafic schist, amphibolite and siliciclastic metasedimentary rocks and a younger succession of metaclastic rocks with an age of ca 500 Ma (Fergusson *et al*. 2001, 2007a). Reconnaissance geochemical data indicate that the mafic schists and amphibolites have MORB-like magmatic affinity within the Bathampton Metamorphics west of Clermont and another suite with an alkaline mafic affinity in the same unit north of Rubyvale (Fig. 3; Withnall *et al*. 1995). Mafic schist and amphibolite with MORB and alkaline magmatic affinities also occur in the northern equivalents of the Anakie Inlier metamorphic succession in the Charter Towers Province of the northern Thomson Fold Belt (Hutton *et al.* 1997; Withnall *et al.* 1997, 2002, 2003; Fergusson *et al*. 2007a, b).

We have made a detailed geochemical study of the tholeiitic suite to the west of Clermont in the Anakie Inlier (Fig. 3) that tests the proposed volcanic passive margin setting of East Gondwana inferred from rock assemblages in southeastern Australia (Direen & Crawford 2003a,b; Crawford *et al*. 2003). We also explore the implications of these data for the reconstruction of the East Gondwana passive margin.

2. Regional Geology

2.1 Thomson Fold Belt and Anakie Inlier

The Anakie Inlier contains exposure of the Thomson Fold Belt in central Queensland. Further west and southwest late Palaeozoic to Cenozoic sedimentary rock cover the basement, but aspects are known from deep basement cores recovered by petroleum companies, deep seismic sections, and gravity and magnetic data (Finlayson 1990; Murray 1994; Wellman 1995). The Thomson Fold Belt mostly contains low-grade siliciclastic metamorphic rock, with steeply dipping bedding, intruded by granites and overlain by various volcanic rocks (Murray 1986, 1994). The Anakie Inlier has an older metamorphic basement, called the Anakie Metamorphic Group, with several units within the southern part (Withnall *et al*. 1995). These rocks record K-Ar ages of ca 500 Ma indicating metamorphism in the Late Cambrian, as also occurs in the Delamerian Orogen of southeastern Australia (Withnall *et al*. 1996). In the southern Anakie Inlier (Withnall *et al.* 1995), the metamorphic basement contains foliated granitic rocks of probable Early Ordovician age. The Anakie Metamorphic Group is faulted against the Fork Lagoons beds, a unit of slate, quartz-rich and lithic sandstone, Upper Ordovician limestone, mafic igneous rocks, and serpentinite. The basement succession is intruded by Devonian granitic rocks and unconformably overlain by Devonian volcanic and sedimentary successions.

2.2 Anakie Metamorphic Group

West of Clermont, the Anakie Metamorphic Group includes several units (Fig. 4; Withnall *et al*. 1995). The basal Bathampton Metamorphics consist of psammitic schist, quartzite, pelitic schist, mafic schist, amphibolite, serpentinite, and calc-silicate rocks, and are overlain by the Rolfe Creek Schist and in turn by the Monteagle Quartzite and then the Wynyard Metamorphics consisting mainly of psammitic schist derived from lithic sandstone. The ages of these units are inferred from U-Pb ages of detrital zircons contained within metaclastic rocks. The Bathampton Metamorphics contain psammite with abundant 1000-1300 Ma zircon ages and a cluster of five grains with a range of 615-665 Ma from two samples indicating a minimum late Neoproterozoic depositional age of ca 600 Ma (Fergusson *et al.* 2001, 2007a). The Wynyard Metamorphics are much younger as one detrital zircon sample gives a range of 510-600 Ma and another sample with detrital monazites gives common ages of ca 540 and 580 Ma. The K-Ar ages on metamorphism and the detrital zircon ages place these rocks as Late Cambrian (Fergusson *et al*. 2001).

The Anakie Metamorphic Group is strongly deformed with the main foliation S_2 flat-lying over much of the region (Withnall *et al*. 1995; Green *et al*. 1998). In the west, the main foliation dips steeply westwards. Deformation is intense with transposition of layering subparallel to S_2. S_1 is only preserved in microlithons and F_2 fold hinges at lower metamorphic grades in the central to eastern area west of Clermont. Metamorphic grade ranges from lower greenschist facies in the east to lower amphibolite facies (andalusite-garnet-staurolite) to the west.

2.3 Bathampton Metamorphics

The Bathampton Metamorphics in the study area west of Clermont consist mainly of psammitic schist and siliceous, pelitic schist in addition to prominent marker horizons of quartzite and mafic schist. Quartzite and mafic schist units outline map-scale F_2 and F_3 folds (Withnall *et al.* 1995; Green *et al*. 1998). Small masses of serpentinite occur within the Bathampton Metamorphics along with marble and calc-silicate rocks too small to show on Fig. 4. Nearly all the mafic schist units occur in the low grade, eastern part where greenschist facies assemblages dominate. They show at least one main foliation (S_2) and in places two foliations (S_1 and S_2). Primary textures are rare with outlines of altered plagioclase crystals present in some samples and rare ghost outlines of microlites in others. Ellipsoidal pods in strongly foliated parts of mafic schists (cf. Bell & Hammond 1984) were mistakenly referred to as pillow lavas in prior studies (Murray 1986 and references therein). Most mafic schists consist of actinolite, chlorite, albite, calcite, quartz, titanite, magnetite and epidote in various combinations and quantities. Muscovite may occur as an additional phase in metasomatised samples.

2.4 Equivalents of the Anakie Metamorphic Group

Equivalents of the Anakie Metamorphic Group are exposed in the Charters Towers Province in the northern-most Thomson Fold Belt and in the Greenvale Province of the southeastern Georgetown Inlier (Fig. 1; Hutton *et al.* 1997; Withnall *et al*. 1995, 1997; Fergusson *et al*. 2007a, b, c). The Charters Towers Province includes a metamorphic basement of the Cape River Metamorphics in the southwest that is dominated by quartzofeldspathic, psammitic rocks associated with mafic schist, amphibolite and intruded by gneissic granitoids of the Fat Hen Creek Complex. This unit was mainly derived from a 1000-1300 Ma igneous source which was possibly an eastward extension of the Musgrave Block of central Australia (Fergusson *et al*. 2007a). Geochemical data from mafic igneous rocks in the Cape River Metamorphics suggest a MORB affinity (Hutton *et al*. 1997). In the northern Charters Towers Province, another basement metamorphic unit, the Argentine Metamorphics, contains an older unit of siliciclastic metasedimentary rocks, derived from a 1000-1300 Ma mainly igneous source, as well as amphibolite and mafic schist. A younger Late Cambrian unit with quartzite, psammite and mafic schist is present (Fergusson *et al.* 2007a, b). The available geochemical data indicate that the mafic igneous rocks of the Argentine Metamorphics consist of a suite with MORB affinity and one of alkaline affinity (Hutton *et al.* 1997; Withnall *et al.* 2002, 2003). Metamorphic rocks from the Greenvale Province include metasedimentary and meta-igneous rocks that are mainly of Late Cambrian to Early Ordovician age and some metasedimentary rocks of late Neoproterozoic age (Fergusson *et al*. 2007c).

3. Geochemistry

3.1 Methods

The study area was mapped in detail at 1:25 000 scale to delineate diverse rock types such as quartzite, psammitic schist and mafic schist (Fig. 4). Samples were selected for geochemical analysis on the basis of minimal alteration although metamorphism and deformation pervade the Bathampton Metamorphics and all samples are altered to some extent. Interpretation of the magmatic affinities of these rocks is therefore based on the immobile elements.

Rock chips were ground to powders in a Tema mill with both tungsten carbide and chrome steel crushers to avoid contamination of some trace elements. Major elements were determined by standard X-ray fluorescence (XRF) methods at the Australian National University and trace elements were determined by a combination of XRF and instrumental neutron activation analysis (INAA) techniques at the Australian National University and Becquerel Laboratories, Lucas Heights, New South Wales, respectively. Seven samples were reanalysed for selected trace elements (Li, Be, Sc, V, Cr, Co, Ni, Cu, Zn, Ga, Rb, Sr, Y, Zr, Nb, Mo, Cd, Sb, Cs, Ba, La, Ce, Pr, Nd, Sm, Eu, Tb, Gd, Dy, Ho, Er, Yb, Lu, Hf, Ta, W, Pb, Th, U) by N. Pearson at the Department of Earth and Planetary Sciences, Macquarie University by inductively coupled plasma-mass spectrometry (ICP-MS). Major and trace element data are given in Table 1.

3. 2 Results

The major and trace element compositions, particularly the light lithophile elements (LILE) are highly variable owing to the intense deformation, alteration and recrystallisation the samples have undergone (Table 1). Much of the variability in major element concentrations is due to variation in content of the high Si-bearing (e.g. quartz, albite) and high CaO-bearing (e.g. calcite, epidote, actinolite) minerals. The high loss on ignition (LOI) recorded in many samples is related to the high content of calcite and mafic (OH)-bearing minerals such as epidote and chlorite that have totally replaced the magmatic minerals. However, despite these effects, consistent and distinctive patterns emerge when immobile elements only are used (Figs. 5 to 8). Further, when a variety of discrimination diagrams involving these immobile elements are applied generally only one particular tectonic setting emerges as subsequently discussed.

Except in Figs. 5 and 6, all data have been plotted on individual diagrams (Figs. 7 to 10). In the former, the data were split into the Yan Can unit (Yan Can Greenstone Member of Withnall *et al.* 1995), the serpentinite unit (Fig. 4) and all other mafic schists outside the Yan Can and serpentinite units (called herein the main unit, Table 1). This division allows for easier interpretation of the diagrams and to ascertain whether the mafic rocks caught up in the serpentinite differ from those in the main and Yan Can Groups.

Zr/TiO_2 and Nb/Y ratios (Zr/TiO_2 = 0.003 – 0.008; Nb/Y = 0.4 – 0.22; Winchester & Floyd 1977; Pearce 1996) clearly indicate that all of the mafic rocks were derived from sub-alkaline, basaltic protoliths. The protoliths resemble low-Ti basalts as Ti/Y values are <400 and Zr/Y values <6 (Erlank *et al.* 1988). TiO_2 is generally <2 wt%. Further, most samples show moderately low $MgO/MgO+FeO^T$ ratios (0.18 – 0.47), Ni (42-154 ppm) and Cr (112-450 ppm) contents (Table 1).

All samples show similar light rare earth element (LREE) depleted patterns with $(Ce/Yb)_N$ varying from 0.45 to 0.96 (x = 0.61; n = 20), $(La/Sm)_N$ from 0.43 to 0.68 (Fig. 5) and have flat heavy rare earth element (HREE) patterns ($[Sm/Lu]_N$ = 0.85-1.33; x = 1.04; n = 11). Rock/MORB patterns show highly variable LILE concentrations but more consistent high field strength element (HFSE) concentrations (Fig. 6). The variability in LILE reflects the mobility of these elements during deformation, alteration and metamorphism. High Th contents appear in some samples (PCW25, PCW28, PCW34, PCW36, PCW38, PCW39, PCW40) but may be unreliable as a value of <1 quoted for many samples analysed by XRF, was taken as 0.99 when constructing rock/MORB figures and using discrimination diagrams (Table 1; Figs. 6, 8). A similar problem arises with Nb where XRF values are quoted as <2. Thus interpretations of patterns incorporating Th and Nb determined by XRF needs caution. If only the HFSE are considered, the patterns are MORB-like.

Application of the discriminant diagrams proposed by Shervais (1982), Cabanis and Lecolle (1989) and Wood (1980) reveal that most samples plot in the N-MORB fields and a few in the volcanic arc basalt field or weakly enriched E-type MORB (Figs. 7, 8). In the Nb/Y - Zr/Y diagram of Fitton *et al.* (1997), the majority cluster around average N-MORB, the minority are either adjacent to mean lower crust (LC) or within the Icelandic array (Fig. 9).

4. Discussion

4.1 Geochemistry

The moderately low $MgO/MgO+FeO^T$ ratios, Ni and Cr contents and moderate TiO_2 contents, imply that fractional crystallization has played a role in determining the composition of the mafic rocks (Table 1). In addition, many show an N-MORB signature (Figs. 5, 6, 7, 8) and a few exhibit volcanic arc basalt field characteristics (Fig. 8). However, these samples along with the remaining samples, plot in the MORB/back-arc basin/continental basalt field of Shervais (1982; Fig. 7), based on their Ti and V contents, confirming their MORB signature.

Although these rocks are MORB-like they are not strictly mid ocean ridge basalts. They have chondrite normalized patterns, $(Sm/Lu)_N$ and $(La/Sm)_N$ values similar to volcanic passive margin basalts (Ludden & Dionne 1992; Fitton *et al.* 1998; Fitton *et al.* 2000). Further, most have lower incompatible trace element contents than N-MORB (e.g. Zr, Nb), a feature of basalts erupted at the onset of continent rifting and sourced from hot oceanic mantle (Ludden & Dionne 1992). They are also associated with meta-sediments of pelitic, psammitic, siliceous and calcareous composition (Withnall *et al.* 1995) which are absent in a mid-ocean ridge setting. These observations suggest that the mafic rocks now exposed in the Clermont area of the Anakie Inlier have come from MORB-like protoliths that have erupted in a strongly attenuated crustal margin setting. However, in contrast to mafic volcanics in volcanic passive margin sequences, they have a restricted extent and have moderately low $MgO/MgO+FeO^T$ values. These features do not support a volcanic passive margin setting but rather a magma-poor rifted margin where melt generation is minimal (e.g. Goban Spur, White 1992; Err and Platta nappes, eastern Central Alps, Schaltegger *et al*. 2002).

4.2 Source

The incompatible element ratios, concentrations and patterns provide a clear indication of the source. They all exhibit LREE depletion indicating a depleted mantle source, while the flat HREE patterns suggest residual garnet was absent in the source. Also, ΔNb (ΔNb = 1.74+log (Nb/Y)-1.92log(Zr/Y): Fitton *et al.* 1997) is <0 for most samples (0.08-0.12; n=2; range=-0.03 to -0.41; n=16; x=-0.19; sd=-0.11), suggesting a N-MORB mantle source. The source may be mixed lithospheric-asthenospheric mantle according to the Nb/La - La/Yb diagram of Abdel-Rahman (2002; Fig. 10). This may be true for most of the samples but three lie within the Iceland array suggesting that they had a plume source.

The high Sc contents and Zr/Sc ratios (range=4.16-0.97; x=1.88; sd=0.67; n=19) are consistent with their derivation from a spinel lherzolite source that has undergone 10-20% melting (Fitton *et al.* 1998) and the Ce/Yb ratios and Ce contents (range=1.7-3.46; x=2.19; sd=0.48; n=11) indicate depths of melt segregation between 10 and 50 km (Ellam 1992). These features suggest that the mafic rocks in the Bathampton Metamorphics represent former basaltic melts derived from a depleted mantle source that were segregated within the spinel lherzolite stability field.

4.3 The East Gondwana margin in northeastern Australia

In northeastern Australia, the East Gondwana passive margin has commonly been located along the Tasman Line of Veevers (1984, 2000), which marks the southward termination of gravity and magnetic anomalies associated with the Palaeo-Mesoproterozoic Mt Isa Inlier (Fig. 1). Mesoproterozoic detrital igneous zircons, however, are abundant in late Neoproterozoic metasedimentary units in northeastern Australia, which implies that this boundary may be the northern margin of an eastern continuation of the central Australian Mesoproterozoic Musgrave Complex (Figs. 1, 2; Fergusson *et al.* 2001, 2007a). Thus the Thomson Fold Belt could overlie Mesoproterozoic crust. This is supported by S-wave seismic data indicating that thick Precambrian crust extends well to the east of the so-called Tasman Line in western Queensland (Kennett *et al.* 2004). The southern extent of the Thomson Fold Belt is commonly depicted along curving gravity and magnetic anomalies in northern New South Wales that possibly mark the boundary with the Palaeozoic accretionary Lachlan Fold Belt (Glen *et al.* 2007).

Late Neoproterozoic and Early Palaeozoic metasedimentary and meta-igneous units of the Anakie Inlier and the Charters Towers Province are affected by intense deformation and low (greenschist facies) to high (amphibolite facies) grade metamorphism (Fergusson *et al.* 2007b). This masks the broad depositional environment, although the abundance of psammitic and pelitic rocks and the presence of small pods of marble are consistent with a marine environment. The original large-scale geometry of the continental margin, however, must have lain close to the present Anakie Inlier and Charters Towers Province. Reconstructions of eastern Australia implying major growth of oceanic complexes in northeastern Australia in the Early Palaeozoic are incorrect (cf. Veevers 1984, 2000; Cawood 2005).

Our data from the southern Anakie Inlier and reconnaissance geochemical studies from mafic meta-igneous rocks in the Charters Towers Province (Withnall *et al*. 1995, 2002, 2003) suggest the East Gondwana margin formed as a magma-poor rifted margin at ca 600 Ma. This accounts for mafic rocks in the Bathampton Metamorphics with a well defined N-MORB-like chemical signature, low $(La/Sm)_N$ values and little contamination by continental crust, features characteristic of igneous rocks in passive margin settings. The age of these rocks is bracketed by psammitic rocks containing detrital zircons with the minimum depositional age of ca 600 Ma and by a younger succession with a depositional age of 500-510 Ma indicated by U-Pb detrital zircon ages and K-Ar ages on the timing of metamorphism (Fergusson *et al.* 2001, 2007a).

4.4 The East Gondwana margin in East Antarctica and southeastern Australia

The reconstruction of the late Neoproterozoic East Gondwana passive margin is helped by limited exposures in the Transantarctic Mountains and by volcanic and marine units in southeastern Australia (Goodge 2002, 2004a; Direen & Crawford 2003a, b). Most of East Antarctica is covered by ice apart from coastal exposures and outcrop in the central Transantarctic Mountains. There the passive margin succession is minor compared to the voluminous Cambrian siliciclastic rocks derived from the 500 to 580 Ma active continental margin (Goodge *et al.* 2002, 2004a, b) and consists mainly of shoreline and shelf sedimentary rocks derived from the East Antarctic shield (Goodge *et al.* 2004a). Rare intrusive rocks in the succession with the U-Pb zircon age of 668 ± 1 Ma on the Cotton Plateau Gabbro provide the only age constraint (Goodge *et al.* 2002).

In southeastern Australia, late Neoproterozoic successions occur in the Wonominta Block of western New South Wales, in the Glenelg Zone of western Victoria, on King Island in western Bass Strait and in western Tasmania (Figs. 1, 2). A volcanic succession of mildly alkaline affinity dated at 586 ± 7 Ma is associated with marine sedimentary rocks in the Wonominta Block of western New South Wales (Crawford *et al.* 1997). As well a younger succession of calcalkaline affinity dated at 525 ± 8 Ma occurs in the Wonominta Block but is substantially younger than the inferred passive margin (Crawford *et al.* 1997). In western Victoria, poorly dated but possibly late Neoproterozoic pillowed rift tholeiitic to transitional alkaline basalts are found in drill core to the north of the exposed Glenelg Zone (Direen & Crawford 2003b; Crawford *et al.* 2003). On King Island, mafic volcanic rocks linked with marine sedimentary rocks are exceptionally thick (>900 m) and are tholeiitic basalts and picrites that have an Nd-Sm isochron age of 579 ± 16 Ma (Meffre *et al.* 2004). Lavas and dykes with transitional alkaline to rift tholeiitic chemistry are widespread in western Tasmania and have latest Neoproterozoic ages of 580-650 Ma (Crawford & Berry 1992; Direen & Crawford 2003a, b).

These mafic volcanic successions are probably far more extensive than their present occurrences would indicate, as they are associated with gravity and magnetic anomalies that are widely developed in Bass Strait, western Victoria, southeastern South Australia and western New South Wales (Direen & Crawford 2003a, b). The major anomalies along the eastern margin of the Delamerian Orogen were assigned to the convergent margin that formed in the Cambrian along the East Gondwana margin (Finn *et al*. 1999). Direen and Crawford (2003a, b) and Meffre *et al.* (2004) interpreted these features as part of a Late Neoproterozoic volcanic passive margin of East Gondwana. They emphasised the presence of picrites and olivine-rich basalts as support for the volcanic passive margin setting.

The contrast between the East Gondwana passive margin in East Antarctica and eastern Australia probably reflects the lack of data from East Antarctica. The age of rifting in East Antarctica hinges on one U-Pb zircon age and is at least 70 m.y. older than the known timing of rifting for eastern Australia. Magmatism in the restricted exposures in the central Transantarctic Mountains is also relatively minor and the passive margin, in contrast to southeastern Australia, has been interpreted as a rifted passive margin (Goodge *et al.* 2004a). This arrangement is reminiscent of the Palaeogene North Atlantic Ocean where well developed volcanic margins adjoining Greenland, Scotland and Norway give way southwards to an older non-volcanic margin with some outlying volcanic regions (Geoffroy 2005).

4.5 East Gondwana margin formation related to Australian intracratonic basins

In the western two thirds of Australia, the Precambrian craton is overlain by many sedimentary basins that include Neoproterozoic to early Palaeozoic successions. These basins help to constrain the Neoproterozoic breakup and formation of the East Gondwana passive margin. Subsidence patterns from these intracratonic basins indicate continent-wide extensional episodes at 900 Ma and at 600 Ma (Lindsay *et al.* 1987), with the younger episode at 600 Ma being related to breakup of a Neoproterozoic continent in Laurentia (Bond *et al.* 1984). This is also consistent with the proposed development of a passive margin in eastern Australia.

Alternatively, several researchers have considered the complex rift history of the intracratonic Adelaide Rift Complex to infer formation of the East Gondwana passive margin. For example, Powell *et al.* (1994) and Preiss (2000) favoured an East Gondwana passive margin at ca 700 Ma. A long history of rifting in the Adelaide Rift Complex includes at least five major episodes between 827 Ma and 525 Ma (Powell *et al.* 1994; Preiss 2000). The ca 700 Ma rift event is associated with the fourth major rift episode in the Adelaide Rift Complex during the Sturtian glaciation, before the first major transgression onto the Gawler Craton, which is regarded as a sag phase of sedimentation following the rift event (Preiss 2000). The only definitive evidence, however, for connection to an ocean to the east is indicated by kilometre-deep erosion channels in the Wonoka Formation (ca 570-580 Ma; Preiss 2000); these were interpreted as submarine canyons by von der Borch *et al*. (1982). These palaeo-canyons are preserved relatively high in the succession and allow for much later formation of the East Gondwana passive margin than often considered (e.g. Pisarevsky *et al.* 2003; Li *et al.* 2008).

In contrast to the evidence for rifting in the Australian craton at 700-900 Ma, such as in the Adelaide Rift Complex, no sign of passive margin development in this interval is known in northeastern Australia. No detrital zircon ages occur in the range 700-900 Ma whereas older and younger detrital zircons abound in the metasedimentary units in northeastern Australia (Fergusson *et al.* 2001, 2007a). Additionally, no compelling evidence for sedimentation in the interval 650 to 900 Ma occurs in northeastern Australia although some successions, such as the predominantly metaclastic rocks of the Cape River Metamorphics are very poorly constrained in age (Fergusson *et al*. 2007a).

4.6 Formation of the East Gondwana margin and the breakup of Rodinia

The breakup history of Rodinia was long and complicated with widespread rifting associated with episodic plume events between ca 825 Ma and 740 Ma (Li *et al.* 2008). The first major breakup event was as early as 750 Ma along the western margin of Laurentia that followed superplume breakout at 780 Ma, as shown by the Gunbarrel event in western Laurentia (Harlan *et al.* 2003). A wide ocean developed between Australia-East Antarctica and South China by ca 720 Ma. Much emphasis has been placed on the inferred superplume-related magmatism and subsequent continental fragmentation as constrained by available palaeomagentic data (Li *et al.* 2008).

In contrast to the ca 825 Ma to 740 Ma timing, earlier analyses of the western Laurentian passive margin and the continental record of extension in Australia favoured fragmentation at ca 600 Ma during the breakup of Rodinia (Bond *et al.* 1984; Lindsay *et al.* 1987). Breakup at ca 600 Ma to form a passive margin in East Gondwana is supported by the geochemistry of the greenstones in northeastern Australia as well as the widely preserved mafic volcanic successions in southeastern Australia (Direen & Crawford 2003b) and by the occurrence of Late Neoproterozoic (Sm-Nd; 562±22Ma), ultramafic-mafic rocks in the Marlborough terrane, New England Orogen, that geochemically suggest an ocean basin setting (Bruce *et al*. 2000).

Of course, both approaches may be consistent as earlier Rodinian fragmentation at 825-740 Ma may have preceded a later rifting event at ca 600 Ma that calved off a microcontinent; a process that is well documented for the Tethyan Ocean (Metcalfe 1996). This would reconcile the evidence for rifting and mafic volcanism at ca 600 Ma in eastern Australia with the absence of evidence for the earlier rifting event. If rifting had occurred earlier, for example at 750 Ma as favoured by Li *et al.* (2008), and was followed by separation of a microcontinent at a younger inboard rift, then the earlier rift-related margin would have been removed as part of the microcontinent and not be preserved in eastern Australia. The fate of the microcontinent after rifting off the East Gondwana margin is unknown. It was possibly a relatively narrow and thin microcontinent (Fig. 11) similar to the Lord Howe Rise and Norfolk Ridge in the Southwest Pacific Ocean that formed with the Tasman Sea. Further, it is possible that the thinner parts of the microcontinent have been subducted and the thicker parts have been dispersed to other parts of the Pacific rim such as China and West Antarctica.

5. Conclusions

Mafic schists in the late Neoproterozoic (ca 600 Ma) Bathampton Metamorphics of the Anakie Inlier in central Queensland, have low TiO_2 (<2%), and incompatible trace element contents. They have depleted LREE and flat, HREE, chondrite normalised patterns. Discrimination diagrams involving immobile elements show that most samples have an N-MORB-like affinity.

The N-MORB magmatic affinity, LREE depleted patterns, low incompatible trace element contents and association with metasedimentary rocks suggest the mafic schists were formed in a magma-poor rifted margin setting. Reconnaissance geochemical data from mafic schist and amphibolite elsewhere in the Anakie Inlier and Charters Towers Province in Queensland also indicate N-MORB and alkaline magmatic affinities supporting this interpretation

Mafic volcanic units in the Anakie Inlier of northeastern Australia at ca 600 Ma are considered to have formed in a magma-poor rifted margin in contrast to mafic volcanic successions of equivalent age in southeastern Australia that developed in a volcanic passive margin setting. This strengthens the suggestion that East Gondwana developed as a rifted and volcanic passive margin in the late Neoproterozoic (Direen & Crawford 2003a, b). The rifting that produced this margin possibly also calved off a microcontinental fragment from eastern Australia and East Antarctica, occurred after the major breakup of Rodinia by as much as 120 m.y. (Li *et al.* 2008).

Acknowledgments

We thank Lin Sutherland for a thorough review of the paper prior to submission. Jiang Zhiyu and Peter Johnson are gratefully acknowledged for drafting of figures. Tim Green acknowledges supervision and support in the field by Paul Carr and Bryan Chenhall at the University of Wollongong. This research was funded from grants from the Australian Research Council, the University of Wollongong and the University of Newcastle. A thought-provoking, incisive review by journal reviewer Cecil Murray has resulted in a substantial improvement to the manuscript. We also thank journal reviewer David Foster and editor Peter Cawood for their review and editorial input respectively.

References

Abdel-Rahman, A.M., 2002. Mesozoic volcanism in the Middle East: geochemical, isotopic and petrogenetic evolution of extension-related alkali basalts from central Lebanon. Geol. Mag. 139, 621-640.

Bell, T.H., Hammond, R.L., 1984. On the internal geometry of mylonite zones. J. Geol. 92, 667-686.

Boger, S.D., Miller, J. McL., 2004. Terminal suturing of Gondwana and the onset of the Ross–Delamerian Orogeny: the cause and effect of an Early Cambrian reconfiguration of plate motions. Earth Planet. Sci. Lett. 219, 35-48.

Bond, G.C., Nickeson, P.A., Kominz, M.A., 1984. Breakup of a supercontinent between 625Ma and 555 Ma: new evidence and implications for continental histories. Earth Planet. Sci. Lett. 70, 325-345.

Bruce, M.C., Niu, Y., Harbort, T.A., Holcombe, R.J., 2000. Petrological, geochemical and geochronological evidence for a Neoproterozoic ocean basin recorded in the Marlborough terrane of the northern New England Fold Belt. Aust. J. Earth Sci. 47, 1053-1064.

Cabanis, B., Lecolle, M., 1989. Le diagramme La/10-Y/15-Nb/8: an outil pour la discrimination des series volcaniques et la mise en evidence des processus de mélange et /ou de contamination crustale. Comptes Rendus de l’Academie des Sciences Series II 309, 2023-2029.

Cawood, P.A., 2005. Terra Australis Orogen: Rodinia breakup and development of the Pacific and Iapetus margins of Gondwana during the Neoproterozoic and Paleozoic. Earth-Sci. Rev. 69, 249-279.

Crawford, A.J., Berry, R.F., 1992. Tectonic implications of Late Proterozoic–Early Palaeozoic igneous rock associations in western Tasmania. Tectonophysics 214, 37-56.

Crawford, A.J., Cayley, R.A., Taylor, D.H., Morand, V.J., Gray, C.M., Kemp, A.I.S., Wohlt, K. E., VandenBerg, A. H. M., Moore, D.H., Maher, S., Direen, N.G., Edwards, J., Donaghy, A.G., Anderson, J.A., Black, L.P., 2003. Neoproterozoic and Cambrian continental rifting, continent-arc collision and post-collisional magmatism. In: Birch, W. (Ed.), The Geology of Victoria, pp. 73-93, Geol. Soc. Aust., Victorian Division.

Crawford, A.J., Stevens, B.P.J., Fanning, C.M., 1997. Geochemistry and tectonic setting of some Neoproterozoic and Early Cambrian volcanics in western New South Wales. Aust. J. Earth Sci. 44, 831-852.

Direen, N.G., Crawford, A.J., 2003a. The Tasman Line: where is it, what is it, and is it Australia’s Rodinian breakup boundary? Aust. J. Earth Sci. 50, 491-502.

Direen, N.G., Crawford, A.J., 2003b. Fossil seaward-dipping reflector sequences preserved in southeastern Australia: a 600 Ma volcanic passive margin in eastern Gondwanaland. J. Geol. Soc. Lond. 160, 985-990.

Ellam, R.M., 1992. Lithospheric thickness as a control on basalt geochemistry. Geology 20, 153-156.
Erlank, A.J., Duncan, A.R., Marsh, J.S., Sweeney, R.J., Hawkesworth, C.J., Milner, S.C., Miller, R.McG., Rogers, N.W., 1988. A laterally extensive geochemical discontinuity in the subcontinental Gondwana lithosphere. In: Geochemical Evolution of the Continental Crust. Conference Abstract, Brazil. 1-10.
Fergusson, C.L., Carr, P.F., Fanning, C.M., Green, T.J., 2001. Proterozoic-Cambrian detrital zircon and monazite ages from the Anakie Inlier, central Queensland: Grenville and Pacific-Gondwana signatures. Aust. J. Earth Sci. 48, 857-866.
Fergusson, C.L., Henderson, R.A., Fanning, C.M., Withnall, I.W., 2007a. Detrital zircon ages in Neoproterozoic to Ordovician siliciclastic rocks, northeastern Australia: implications for the tectonic history of the East Gondwana continental margin. J. Geol. Soc. Lond. 164, 215-225.
Fergusson, C.L., Henderson, R.A., Withnall, I.W., Fanning, C.M., Phillips, D., Lewthwaite, K.J., 2007b. Structural, metamorphic and geochronological constraints on alternating compression and extension in the Early Paleozoic Gondwanan Pacific margin, northeastern Australia. Tectonics 26, TC3008, doi:10.1029/2006TC001979.
Fergusson, C.L., Henderson, R.A., Withnall, I.W., Fanning, C.M., 2007c. Structural history of the Greenvale Province, north Queensland: Early Palaeozoic extension and convergence on the Pacific margin of Gondwana. Aust. J. Earth Sci. 54, 573-595.
Finlayson, D.M. (Ed.), 1990. The Eromanga-Brisbane Geoscience Transect: a guide to basin development across Phanerozoic Australia in southern Queensland. Bureau of Mineral Resources, Geology and Geophysics, Bulletin 232, Canberra.
Finn, C., Moore, D., Damaske, D., Mackey, T., 1999. Aeromagnetic legacy of early Paleozoic subduction along the Pacific margin of Gondwana. Geology 27, 1087-1090.
Fitton, J.G., Saunders, A.D., Norry, M.J., Hardarson, B.S., Taylor, R.N., 1997. Thermal and chemical structure of the Iceland plume. Earth Planet. Sci. Lett. 153, 197-208.
Fitton, J.G., Saunders, A.D., Larsen, L.M., Hardarson, B.S., Norry, M.J., 1998. Volcanic rocks from the southeast Greenland margin at 63^{o}N: composition, petrogenesis, and mantle sources. In: Saunders, A.D., Larsen, H.C., Wise, S.W. (Eds.), Proceedings of the Ocean Drilling Program, Scientific Results 152, pp. 331-350. College Station, TX (Ocean Drilling Program).
Fitton, J.G., Larsen, L.M., Saunders, A.D., Hardarson, B.S., Kempton, P.D., 2000. Paleogene Continental to Oceanic Magmatism on the SE Greenland Continental Margin at 63^{o}N: a review of the Results of Ocean Drilling Program Legs 152 and 163. J. Petrology 41, 951-966.
Fitzsimons, I.C.W., 2003. Proterozoic basement provinces of southern and southwestern Australia, and their correlation with Antarctica. In: Yoshida, M., Windley, B. F., Dasgupta, S. (Eds.), Proterozoic East Gondwana: Supercontinent Assembly and Breakup. Geol. Soc. Lond. Spec. Publ. 206, pp. 93-130.
Geoffroy, L., 2005. Volcanic passive margins. C. R. Geoscience 337, 1395-1408.
Glen, R.A., Poudjom Djomani, Y., Korsch, R.J., Costello, R.D., Dick, S., 2007. Thomson-Lachlan seismic project – results and implications. Mineral Exploration in the Tasmanides, Mines and Wines 2007, Australian Institute of Geoscientists Bulletin 46, pp. 73-78. http://www.smedg.org.au/M&W2007Abs.pdf
Green, T.J., Fergusson, C.L., Withnall, I.W., 1998. Refolding and strain in the Neoproterozoic Early Palaeozoic Anakie Metamorphic Group, central Queensland. Aust. J. Earth Sci. 45, 915-924.

Goodge, J.W., Myrow, P., Williams, I.S., Bowring, S.A., 2002. Age and provenance of the Beardmore Group, Antarctica: constraints on Rodinia supercontinent breakup. J. Geol. 110, 393-406.

Goodge, J.W., Williams, I.S., Myrow, P., 2004a. Provenance of Neoproterozoic and lower Paleozoic siliciclastic rocks of the central Ross Orogen, Antarctica: Detrital record of rift-, passive- and active-margin sedimentation. Geol. Soc. Am. Bull. 116, 1253-1279.

Goodge, J.W., Myrow, P., Phillips, D., Fanning, C.M., Williams, I.S., 2004b. Siliciclastic record of rapid denudation in response to convergent-margin orogenesis, Ross Orogen, Antarctica. In: Bernet, M., Spiegel, C. (Eds.), Detrital thermochronology—Provenance analysis, exhumation, and landscape evolution of mountain belts, pp. 105-126. Geol. Soc. Amer. Spec. Pap. 378.

Harlan, S.S., Heaman, L., LeCheminant, A.N., Premo, W.R., 2003. Gunbarrel mafic magmatic event: a key 780 Ma time marker for Rodinia plate reconstructions. Geology 31, 1053-1056, DOI: 10.1130/G19944.1.

Hutton, L.J., Draper, J.J., Rienks, I.P., Withnall, I.W., Knutson, J., 1997. Chapter 6. Charters Towers region. In: Bain, J.H.C., Draper, J.J. (Eds.), North Queensland Geology, pp. 165-224. Australian Geological Survey Organisation Bulletin 240 and Queensland Geology 9.

Kennett, B.L.N., Fishwick, S., Reading, A.M., Rawlinson, N., 2004. Contrasts in mantle structure beneath Australia: relation to Tasman Lines? Aust. J. Earth Sci. 51, 563-569.

Li, Z.X., Bogdanova, S.V., Collins, A.S., Davidson, A., De Waele, B., Ernst, R.E., Fitzsimons, I.C.W., Fuck, R.A., Gladkochub, D.P., Jacobs, J., Karlstrom, K.E., Lul, S., Natapovm, L.M., Pease, V., Pisarevsky, S.A., Thrane, K., Vernikovsky, V., 2008. Assembly, configuration, and break-up history of Rodinia: a synthesis. Precambrian Res. 160, 179-210.

Lindsay, J.F., Korsch, R.J., Wilford, J.R., 1987. Timing the breakup of a Proterozoic supercontinent: evidence from Australian intracratonic basins. Geology 15, 1061-1064.

Ludden, J.N., Dionne, B., 1992. The geochemistry of oceanic crust at the onset of rifting in the Indian Ocean. In: Gradstein, F.M., Ludden, J.N. (Eds.), Proceedings of the Ocean Drilling Program Scientific Results 123, College Station, TX, (Ocean Drilling Program), pp. 791-799.

Meffre, S., Direen, N.G., Crawford, A.J., Kamenetskya, V., 2004. Mafic volcanic rocks on King Island, Tasmania: evidence for 579 Ma break-up in east Gondwana. Precambrian Res. 135, 177-191.

Metcalfe, I., 1996. Gondwanaland dispersion, Asian accretion and evolution of eastern Tethys. Aust. J. Earth Sci. 43, 605-623.

Müller, R.D., Gaina, C., Clark, S., 2000. 5 Seafloor spreading around Australia. In: Veevers, J.J. (Ed.), Billion-year earth history of Australia and neighbours in Gondwanaland. GEMOC Press, Sydney, pp. 18-28.

Murray, C.G., 1986. Metallogeny and tectonic development of the Tasman Fold Belt System in Queensland. Ore Geol. Rev. 1, 315-400.

Murray, C.G., 1994. Basement cores from the Tasman Fold Belt system beneath the Great Artesian Basin in Queensland. Department of Minerals and Energy, Queensland Geological Record 1994/10, 96 pp.

Pearce, J.A., 1996. A user's guide to basalt discrimination diagrams. In: Wyman, D.A. (Ed.), Trace element geochemistry of volcanic rocks: applications for massive sulphide exploration. Geological Association of Canada, Short Course Notes, 12, pp. 79-113.

Pisarevsky, S.A., Wingate, M.T.D., Powell, C.McA., Johnson, S., Evans, D.A.D., 2003. Models of Rodinia assembly and fragmentation. In: Yoshida, M., Windley, B.F., Dasgupta, S. (Eds.), Proterozoic East Gondwana: Supercontinent Assembly and Breakup, pp. 35-55. Geol. Soc. Lond., Spec. Publ. 206.

Powell, C.McA., Preiss, W.V., Gatehouse, C.G., Krapez B., Li, Z.X., 1994. South Australian record of a Rodinian epicontinental basin and its mid-Neoproterozoic breakup (~700 Ma) to form the Palaeo-Pacific Ocean. Tectonophysics 237, 112-140.

Preiss, W.V., 2000. The Adelaide Geosyncline of South Australia and its significance in Neoproterozoic continental reconstruction. Precambrian Res. 100, 21-63.

Schaltegger, U., Desmurs, L., Manatschal, G., Muntener, O., Meier, M., Frank, M., Bernoulli, D., 2002. The transition from rifting to sea-floor spreading within a magma-poor rifted margin: field and isotropic constraints. Terra Nova 14, 156-162.

Shervais, J.W., 1982. Ti-V plots and the petrogenesis of modern and ophiolitic lavas. Earth Planet. Sci. Lett. 59, 101-118.

Sun, S-S., McDonough, W.F., 1989. Chemical and isotopic systematics of oceanic basalts: implications for Mantle Compositions and Processes. In: Saunders, A.D., Norry, M.J. (Eds.), Magmatism in the Ocean Basins, pp. 315-345. Geol. Soc. Lond. Spec. Publ. 42.

Veevers, J.J. (Ed.), 1984. Phanerozoic earth history of Australia.Clarendon Press, Oxford.

Veevers, J.J. (Ed.), 2000. Billion-year earth history of Australia and neighbours in Gondwanaland. GEOMOC Press, Sydney.

Veevers, J.J., Walter, M.R., Scheibner, E., 1997. Neoproterozoic tectonics of Australia-Antarctica and Laurentia and the 560 Ma birth of the Pacific Ocean reflect the 400 m.y. Pangean Supercycle. J. Geol. 105, 225-242.

von der Borch, C.C., Smit, R., Grady, A.E., 1982. Late Proterozoic submarine canyons of Adelaide geosyncline, South Australia. Am. Assoc. Petrol. Geol. Bull. 66, 332-347.

Wellman, P., 1995. Tasman Orogenic System: a model for its subdivision and growth history based on gravity and magnetic anomalies. Econ. Geol. 90, 1430-1442.

White, R.S., 1992. Magmatism during and after continental break-up. In: Storey, B.C., Alabaster, T., Pankhurst, R.J. (Eds.), Magmatism and the Causes of Continental Break-up, pp. 1-16, Geol. Soc., Lond., Spec. Publ. 86.

Winchester, J.A., Floyd, P.A., 1977. Geochemical discrimination of different magma series and their differentiation products using immobile elements. Chem. Geol. 20, 325-343.

Wingate, M.T.D., Campbell, I.H., Compston, W., Gibson, G.M., 1998. Ion-probe U–Pb ages for Neoproterozoic basaltic magmatism in south-central Australia and implications for the breakup of Rodinia. Precambrian Res. 87, 135-159.

Withnall, I.W., Blake, P.R., Crouch, S.B.S., Tenison Woods, K., Hayward, M.A., Lam, J.S., Garrad, P., Rees, I.D., 1995. Geology of the southern part of the Anakie Inlier, central Queensland. Queensland Geology 7.

Withnall, I.W., Golding, S.D., Rees, I.D., Dobos, S.K., 1996. K-Ar dating of the Anakie Metamorphic Group: evidence for an extension of the Delamerian Orogeny into central Queensland. Aust. J. Earth Sci. 43, 567-572.

Withnall, I.W., MacKenzie, D.E., Denaro, T.J., Bain, J.H.C., Oversby, B.S., Knutson, J., Donchak, P.J.T., Champion, D.C., Wellman, P., Cruikshank, B.I., Sun, S.S., Pain, C.F., 1997. Chapter 3. Georgetown Region. In: Bain, J.H.C., Draper, J.J. (Eds.), North Queensland Geology, pp. 19-116. Australian Geological Survey Organisation Bulletin 240 and Queensland Geology 9.

Withnall, I.W., Hutton, L.J., Garrad, P.D., Jones, M.R., Blight, R.K.J., 2002. North Queensland Gold and Base Metal Study Stage 1– Georgetown GIS. Geological Survey of Queensland, Department of Natural Resources and Mines, digital data (including explanatory notes) released on CD-ROM.

Withnall, I.W., Hutton, L.J., Blight, R.K.J., 2003. North Queensland Gold and Base Metal Study Stage 2 – Charters Towers GIS. Geological Survey of Queensland, Department of Natural Resources and Mines, digital data (including explanatory notes) released on CD-ROM.

Wood, D.A., 1980. The application of a Th-Hf-Ta diagram to problems for tectonomagmatic classification and to establishing the nature of crustal contamination of basaltic lavas of the British Tertiary volcanic province. Earth Planet. Sci. Lett. 50, 11-30.

Figures

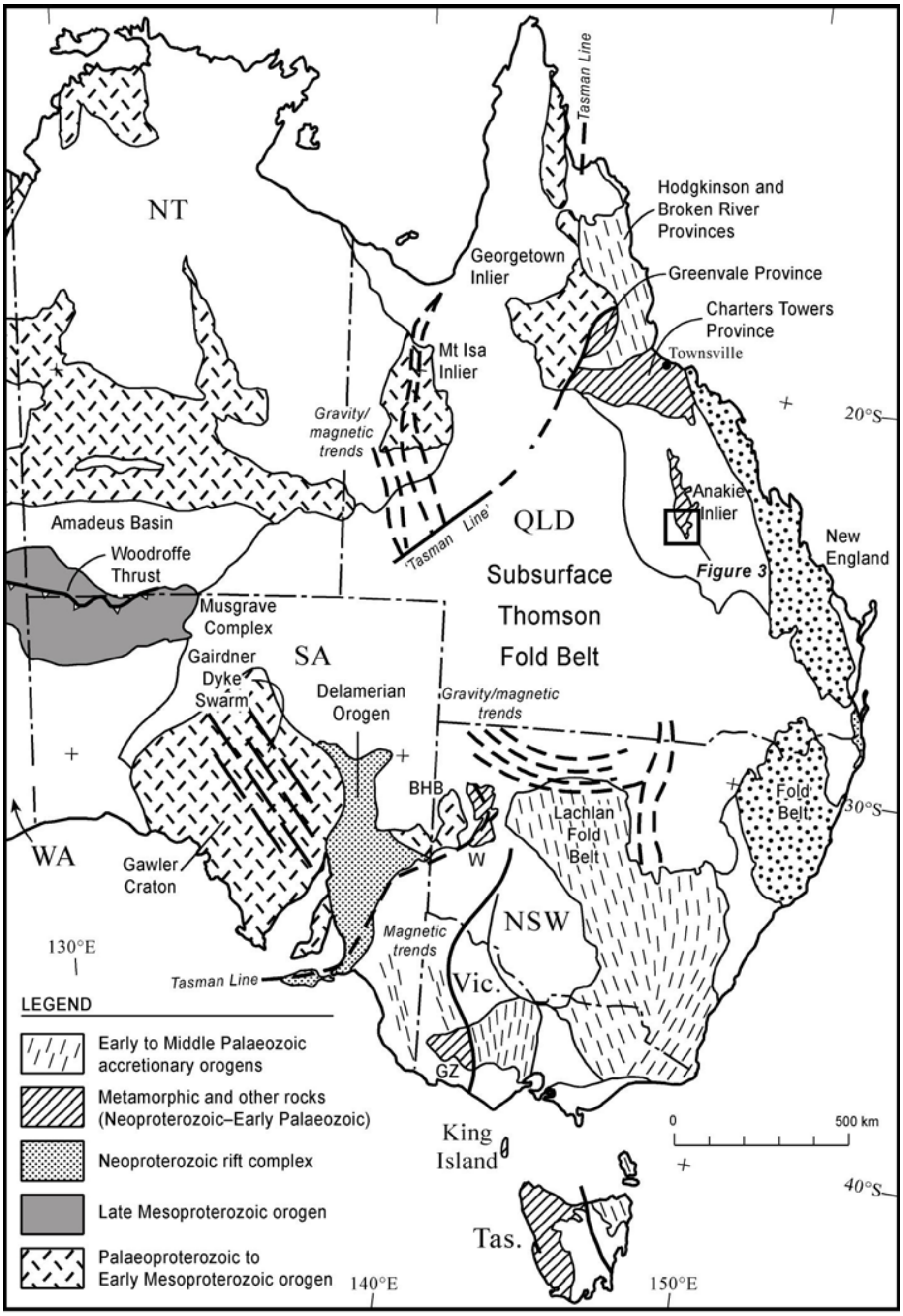

Figure 1

Fig. 1. Map of the main geophysical and geological features of central and eastern Australia related to the eastern Neoproterozoic to Early Palaeozoic margin of East Gondwana. The Tasman Line is commonly regarded as the eastern boundary of Palaeoproterozoic–Mesoproterozoic orogens (Mt Isa, Georgetown, Broken Hill) in eastern Australia (Veevers 1984, 2000). Abbreviations: BHB = Broken Hill Block, GZ = Glenelg Zone, W = Wonominta

Block. Delamerian Orogen includes Wonominta Block, Glenelg Zone and western Tasmania. Unpatterned area is all post-Ordovician to Recent cover. The boundary between the Lachlan and Thomson Fold Belts is poorly defined due to lack of exposure and commonly placed within the curving gravity and magnetic trends in northern New South Wales.

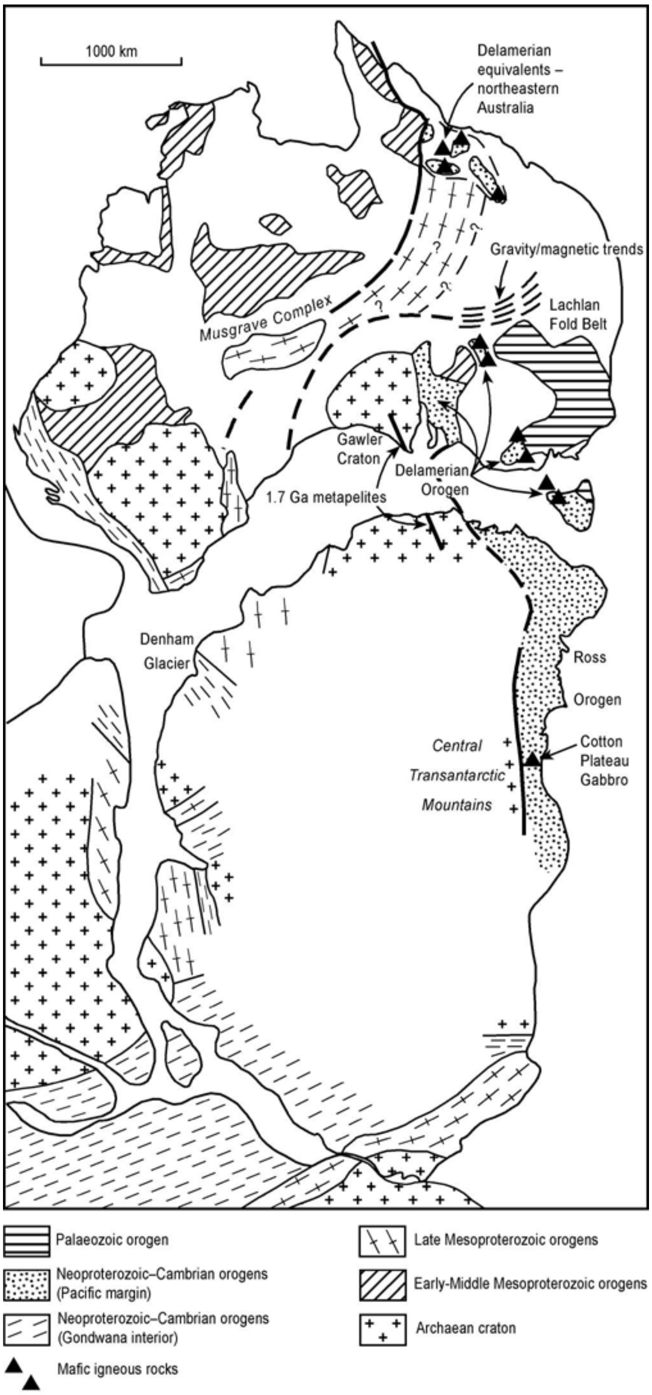

Figure 2

Fig. 2. Major basement units of East Gondwana (reconstructions after Müller *et al.* 2000; Fitzsimons 2003; Boger & Miller 2004). Note reconstruction of Australia and East Antarctica is tightly constrained by the 1.7 Ga metapelite marker in the Gawler Craton and the metamorphic basement of King George V Land. Postulated eastern (subsurface) extension of the Musgrave Complex is shown into northeastern Australia (Fergusson *et al.* 2007a).

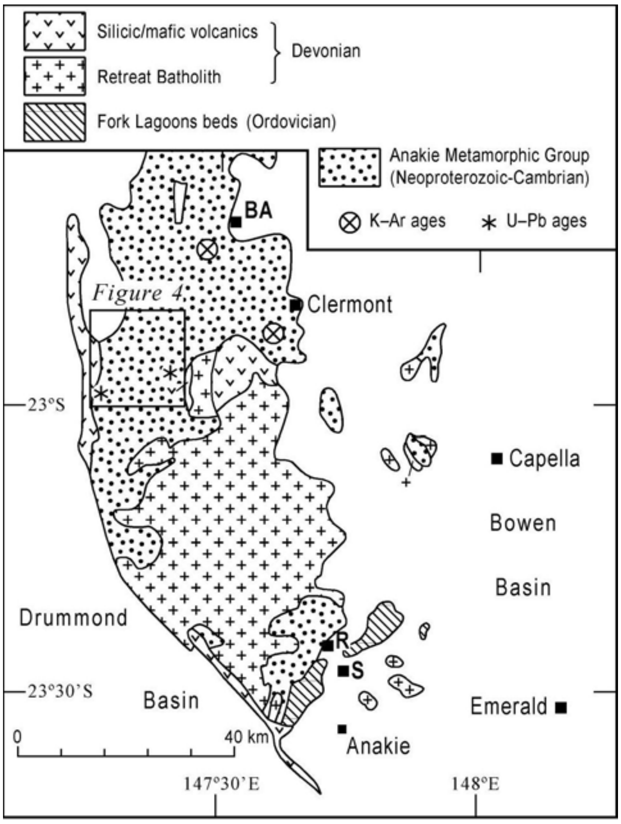

Fig. 3. Map of the southern Anakie Inlier with mainly pre-Carboniferous units shown (see Fig. 1 for location, after Withnall *et al.* 1995). K-Ar age sites have been obtained from Withnall *et al.* (1996) and U-Pb age sites from Fergusson *et al.* (2001). BA = Blair Athol, R = Rubyvale, S = Sapphire.

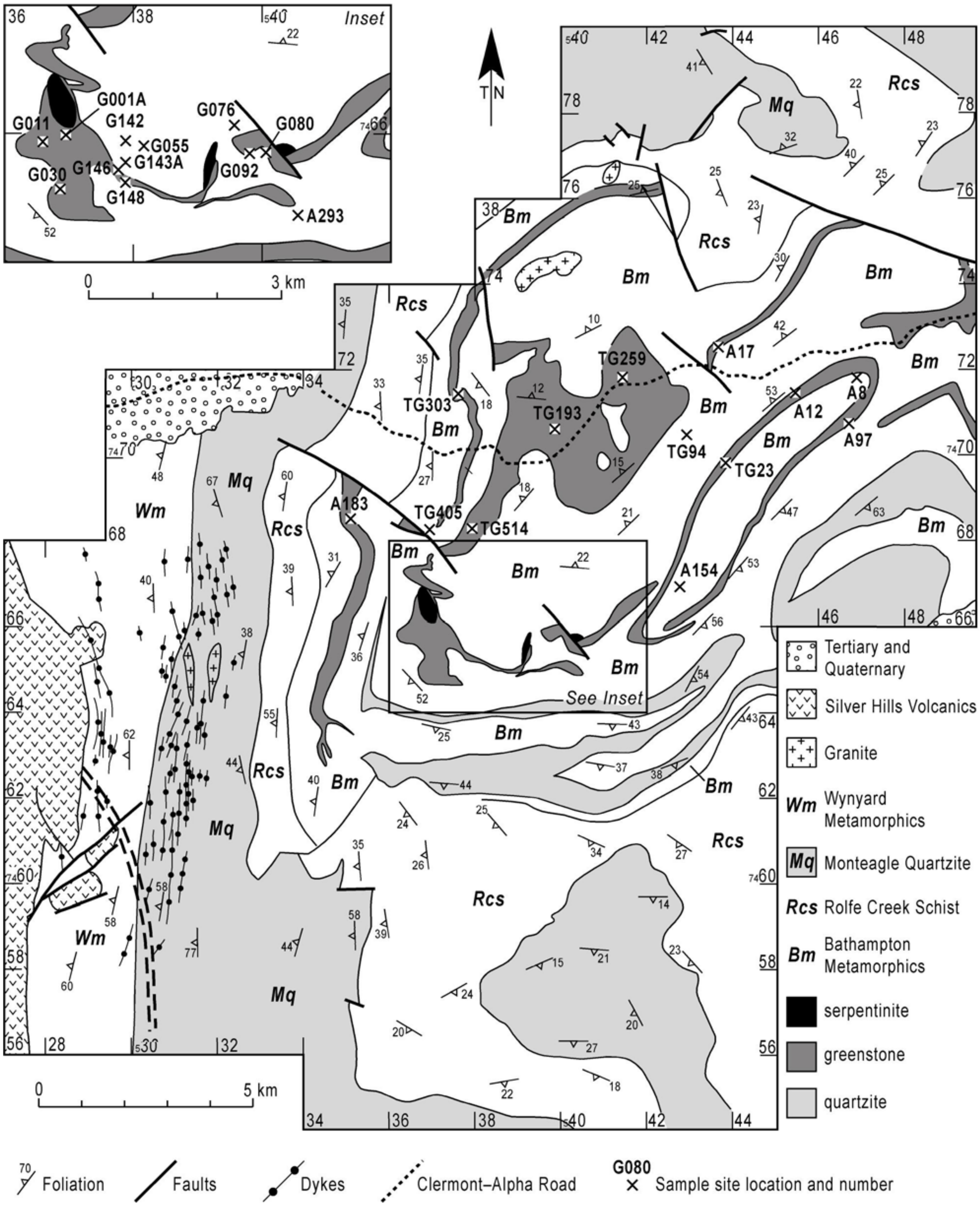

Fig. 4. Map of the study area to the west of Clermont (see Fig. 3 for location) showing the main lithological units along with larger greenstone and quartzite subunits of the Bathampton Metamorphics (modified on the basis of new mapping from Withnall *et al.* 1995). Sample locations are given for mafic schist samples (see field numbers in Table 1).

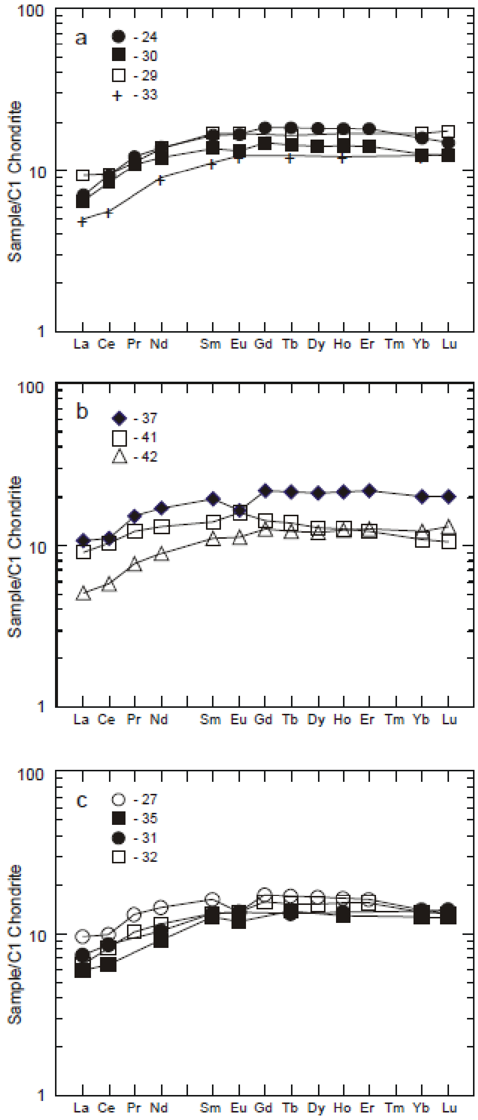

Fig. 5. Chondrite normalized rare earth patterns of samples. (a) Main group (see PCW numbers in Table 1). (b) Serpentinite group. (c) Yan Can group. Note that all are LREE-depleted. Normalizing values from Sun and McDonough (1989).

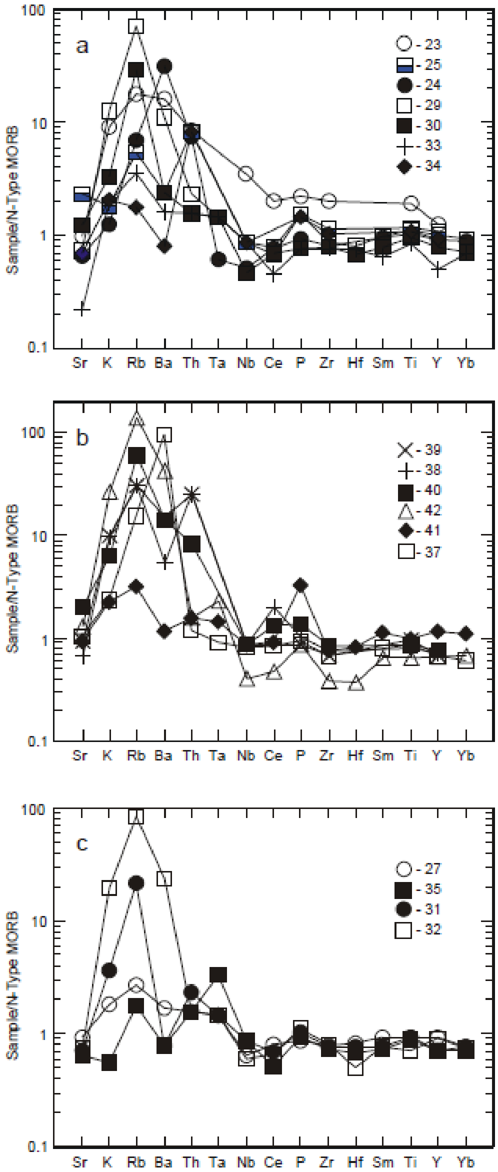

Fig. 6. Rock-MORB normalization diagrams. (a) Main group (see PCW numbers in Table 1). (b) Serpentinite group. (c) Yan Can group. Normalizing values from Sun and McDonough (1989).

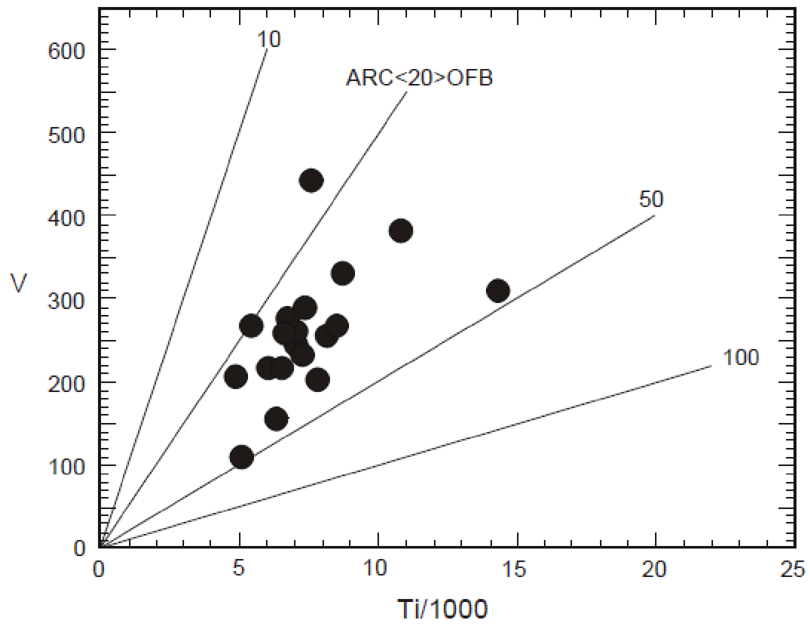

Fig. 7. V-Ti diagram of Shervais (1982) showing that all but one sample plots in the MORB, back-arc basin and continental basalt field. ARC-Arc tholeiite; OFB-Ocean floor basalt. <50Ti/V>20-MORB/Back-arc basin/Continental flood basalt field; Ti/V> 50-Ocean-island and alkali basalt field.

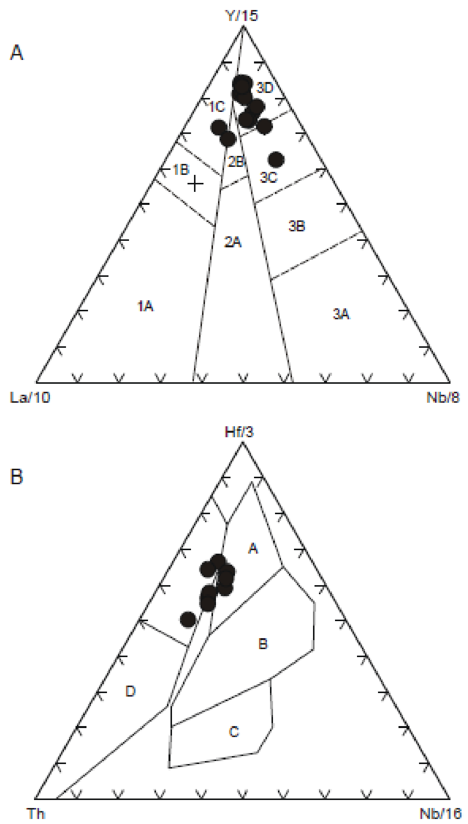

Fig. 8. (a) Y/15-La/10-Nb/8 discrimination diagram of Cabanis and Lecolle (1989). 1-Volcanic arc basalts; 2A-Continental basalts; 2B- Back-arc basalts; 3A- Alkaline basalts from intercontinental rift; 3B, 3C E-type MORB (3B enriched; 3C weakly enriched; 3D-N-type

MORB). Note: not all samples could be plotted because they had compositions similar to those shown. (b) Hf/3-Th-Nb/16 discrimination diagram of Wood (1980). A - N-type MORB; B-E-type MORB; C-Alkaline within plate basalts. D-volcanic arc basalts (Island arc tholeiites plot in field D where Hf/Th >3).

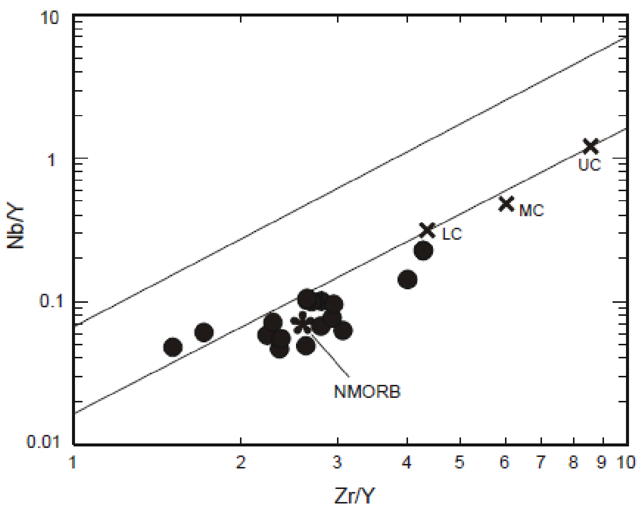

Fig. 9. Nb/Y-Zr/Y diagram of Fitton *et al.* (1997). Parallel lines define the upper and lower bounds of the Iceland array. LC-lower crust; MC-middle crust; UC-upper crust. Note that the majority of the samples cluster around NMORB. Two plot close to LC.

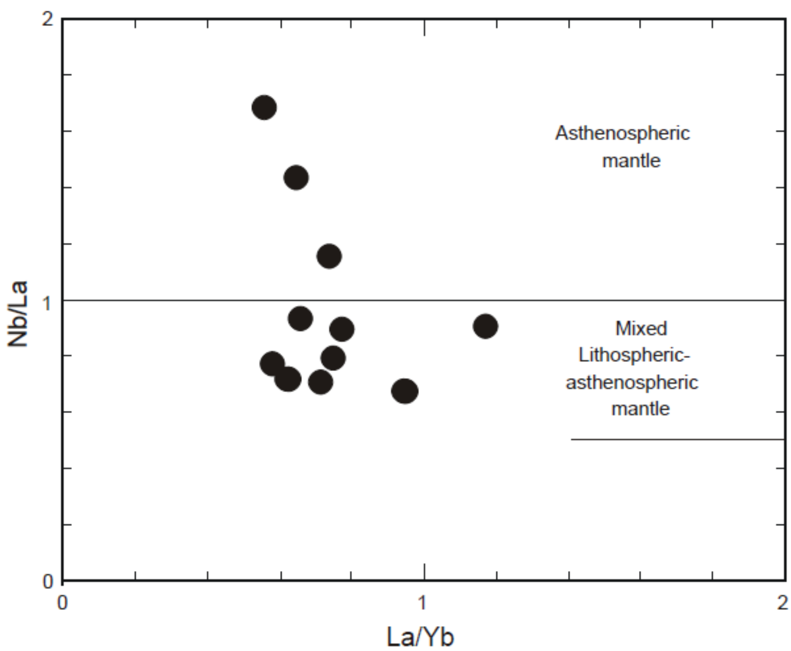

Fig. 10. Nb/La - La/Yb diagram of Abdel-Rahman (2002). Note that because of overlap problems not all data can be shown. Also note that the three samples that have Nb/La ratios >1 have Nb values of <2 according to XRF analysis. A value of 1.99 has been used to plot them on this diagram. This may be greater than the true value and therefore may indicate an incorrect source. See text for discussion.

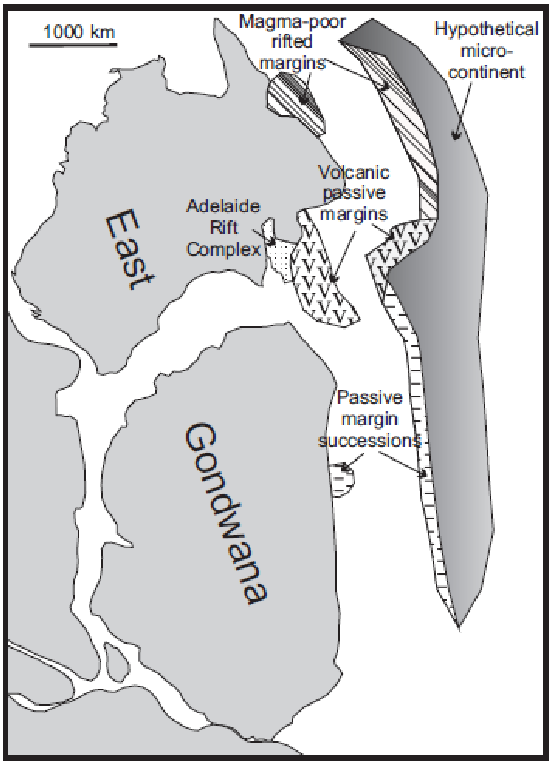

Fig. 11. Reconstruction of the East Gondwana passive margin and the hypothetical microcontinent at ca 560 Ma after rifting.

Table Caption

Table 1. Major and trace element analyses of mafic schists, Bathampton Metamorphics.

Table 1 Major and trace element analyses of mafic schists, Bathampton Metamorphics — Whole rock analyses of mafic rocks.

Sample number	PCW23	PCW24	PCW25	PCW29	PCW30	PCW33	PCW34	PCW28	PCW36	PCW37	PCW38	PCW39	PCW40	PCW41	PCW42	PCW27	PCW31	PCW32	PCW35
Field Number	A12	A17	A97	TG23	TG94	TG303	TG405	A293	G001A	G011	G030	G055	G076	G092	G142A	A183*	TG198	TG259	TG514
Rock Number	R15530	R15531	R15532	R15536	R15537	R15540	R15541	R15535	R15543	R15544	R15545	R15546	R15547	R15548	R15549	R155817	R15538	R15539	R15542
Units	Main	Main	Main	Main	Main	Main	Main	Serp	Serp	Serp	Serp	Serp	Serp	*Serp*	Serp	Yan Can	Yan Can	Yan Can	Yan Can
Grid reference	8352-	8352-	8352-	8352-	8352-	8352-	8352-	8352-	8352-	8352-	8352-	8352-	8352-	*8352-*	8352-	8352-	8352-	8352-	8352-
	451716	436723	468709	436699	430707	376715	370681	405648	369661	365659	368651	381660	395662	395655	379660	349685	398707	413718	379685
SiO_2	51.78	46.13	46.97	44.96	43.02	61.94	44.11	21.80	22.91	36.05	39.43	40.25	49.37	43.62	47.25	48.66	42.83	39.79	48.05
TiO_2	2.32	1.17	1.41	1.28	1.06	1.04	1.30	0.62	1.48	1.16	0.88	1.08	1.03	0.97	0.71	1.14	1.03	0.80	1.13
Al_2O_3	14.86	13.05	13.85	14.63	12.07	12.32	14.13	5.75	17.68	15.39	12.37	12.88	12.61	13.75	10.97	15.43	12.42	14.22	15.54
Fe_2O_3	14.03	10.81	11.43	11.68	9.08	7.56	12.04	5.93	11.93	11.43	8.77	10.96	10.16	9.26	7.37	10.24	9.75	7.49	10.53
MnO	0.15	0.15	0.17	0.14	0.14	0.12	0.21	0.26	0.20	0.25	0.16	0.17	0.22	0.12	0.14	0.15	0.15	0.13	0.14
MgO	3.32	6.76	3.93	5.14	5.52	4.57	6.02	5.20	6.83	1.79	7.50	5.22	2.19	6.87	3.15	8.65	5.49	2.82	5.40
CaO	5.19	8.37	16.88	7.37	12.92	6.46	14.94	31.88	18.01	23.29	13.86	12.61	16.15	11.73	13.91	9.48	12.18	18.73	18.11
Na_2O	4.47	3.27	1.71	3.73	3.34	4.06	2.55	1.33	0.25	1.63	3.00	3.93	0.79	2.44	2.35	3.18	2.63	2.18	0.43
K_2O	0.63	0.08	0.12	0.81	0.21	0.14	0.14	0.03	2.55	0.15	0.61	0.63	0.42	0.15	1.67	0.13	0.23	1.24	0.04
P_2O_5	0.25	0.10	0.17	0.16	0.08	0.09	0.16	0.16	0.19	0.35	0.10	0.09	0.15	0.10	0.09	0.10	0.10	0.11	0.11
Rest	0.16	0.18	0.18	0.18	0.15	0.11	0.18	0.08	0.24	0.17	0.18	0.16	0.17	0.23	0.15	0.16	0.12	0.13	0.14
LOI	2.01	9.71	3.46	9.70	13.26	1.75	5.45	27.59	18.49	9.67	13.46	12.42	7.62	11.11	12.74	3.18	13.17	13.25	1.59
Total	99.17	99.78	100.28	99.78	100.85	100.16	101.23	100.63	100.76	101.33	100.32	100.40	100.88	100.35	100.50	100.50	100.10	100.89	101.21
								Trace elements											
Ba	100	*198*	15	70	*15*	10	5	5	425	*7.38*	35	95	90	*608*	*264*	*10.7*	4.99	*151*	4.99
Rb	10	*3.83*	3	40	*16.1*	2	1	1	49	*1.78*	17	17	34	*8.60*	*79.1*	*1.5*	12	*47.2*	0.99
Sr	89	*58.9*	207	66	*110.6*	20	62	123	164	*83.9*	61	85	182	*94.1*	*117.4*	*83*	64	*67.7*	58
Pb	<2	*0.758*	2	<2	*1.15*	<2	<2	4	26	*0.663*	2	2	8	*2.04*	*5.92*	*0.73*	<2	*0.746*	2
Th	1	*0.89*	0.99	**0.28**	**<0.2**	**<0.2**	0.99	0.99	3	**<0.2**	3	3	1	*0.143*	**<0.2**	**<0.2**	**0.28**	**<0.2**	**<0.2**
U	<1	*0.06*	<1	<1	*0.045*	<1	<1	<1	<1	*0.10*	1	1	<1	*0.053*	*0.083*	*0.072*	<1	*0.09*	<1
Zr	150	60	84	64	58	56	76	32	98	56	56	50	62	50	28	58	56	60	54
Nb	8	*1.2*	2	2	*1.09*	2	2		2	*2.0*	2	2	2	*1.93*	*0.94*	*1.5*	2	*1.4*	2
Y	35	*25.5*	30	28	*22.1*	14	26	18	32	*32.7*	20	19	21	*19*	*18.6*	*26*	20	*25.4*	20
La	4	*1.67*		**2.22**	*1.53*	**1.18**		2	6	*2.53*	8	2	4	*2.14*	*1.20*	*2.23*	**1.72**	*1.5*	**1.39**
Ce	15	*5.69*	5	**5.81**	*5.16*	**3.41**			20	*6.75*	15		10	*6.33*	*3.52*	*5.99*	**5.16**	*4.91*	**3.88**
Pr		*1.14*			*1.02*					*1.43*				*1.15*	*0.72*	*1.23*		*0.962*	
Nd		*6.40*		**6.39**	*5.59*	**4.22**				*7.88*				*6.04*	*4.13*	*6.61*	**4.80**	*5.33*	**4.22**
Sm		*2.51*		**2.58**	*2.07*	**1.71**				*2.94*				*2.11*	*1.68*	*2.44*	**2.01**	2.02	**1.90**
Eu		*0.952*		**0.98**	*0.765*	**0.71**				*0.947*				*0.913*	*0.648*	*0.781*	**0.78**	*0.773*	**0.68**
Tb		*0.681*		**0.61**	*0.535*	**0.46**				*0.794*				*0.504*	*0.454*	*0.629*	**0.49**	*0.562*	**0.51**
Gd		*3.77*			*3.03*					*4.44*				*2.90*	*2.56*	*3.510*		*3.16*	
Dy		*4.53*			*3.55*					*5.31*				*3.240*	*3.04*	*4.170*		*3.81*	
Ho		*1.01*		**0.96**	*0.795*	**0.69**				*1.20*				*0.707*	*0.691*	*0.923*	**0.76**	*0.867*	**0.72**
Er		*2.95*			*2.32*					*3.56*				*2.00*	*2.07*	*2.650*		*2.52*	
Yb		*2.68*		**2.87**	*2.14*	**2.09**				*3.38*				*1.83*	*2.07*	*2.350*	**2.31**	*2.28*	**2.14**
Lu		*0.377*		**0.44**	*0.311*	**0.32**				*0.508*				*0.263*	*0.328*	*0.332*	**0.35**	*0.331*	**0.32**
Sc	36	*31.7*	46	36	*30*	28	42	12	58	*29.2*	30	50	26	*35.6*	*28.8*	*43*	34	*31.9*	*35*
V	310	*203*	330	268	*234*	156	256	110	382	*443*	216	290	258	*218*	*211*	*245*	260	*268*	278
Cr	144	*287*	284	350	*211*	224	444	112	212	*152*	450	284	274	*335*	*138*	*415*	178	*219*	266
Ni	66	*106*	112	134	*75.7*	76	142	62	144	*90*	154	84	98	*89*	*42.1*	*98*	52	*50.6*	66
Cu	54	*31.5*	16	58	*139*	40	80	30	8	*54.8*	100	44	52	*103*	*93.1*	*76.3*	54	*144*	34
Zn	100	*60.3*	62	92	*46*	82	94	58	82	*25.2*	76	92	62	*53.1*	*31.4*	*69.1*	64	*40.8*	68
Sn	5		5				5		5	*10*			5					5.0	5
Ga	16	*10.4*	17	14	*12.5*	11	16	7	16	*24*	14	15	16	*12.4*	*11.3*	*13.1*	13	*30*	21
As	2	*12*	2	2	*3*				1	*5*	1	1	5						
Hf				**1.66**	**1.39**	**1.52**				**1.66**					**0.77**	**1.69**	**1.57**	**1.02**	**1.38**
Ta		*0.08*		**<0.2**	**<0.2**	**<0.2**				**<0.2**				*0.119*	**0.30**	**<0.2**	**<0.2**	**<0.2**	**0.43**

Note: values in italics have been determined by ICPMS, those in bold by INAA. LOI-Loss on Ignition.